The Journal of Arthroplasty xxx (2015) xxx–xxx

Contents lists available at ScienceDirect

The Journal of Arthroplasty

journal homepage: www.arthroplastyjournal.org

Intraoperative Periprosthetic Femur Fracture: A Biomechanical Analysis of Cerclage Fixation

Nicholas B. Frisch, MD, MBA [a], Michael A. Charters, MD, MS [a], Jakub Sikora-Klak, BS [b], Richard F. Banglmaier, PhD [a], Daniel J. Oravec, M.S. [c], Craig D. Silverton, DO [a]

[a] Henry Ford Health System Department of Orthopaedic Surgery, Detroit, Michigan
[b] Wayne State University School of Medicine, Detroit, Michigan
[c] Bone and Joint Center, Henry Ford Hospital, Detroit, Michigan

ARTICLE INFO

Article history:
Received 8 August 2014
Accepted 21 February 2015
Available online xxxx

Keywords:
total hip arthroplasty
periprosthetic fracture
revision
complication
cerclage
fixation

ABSTRACT

Intraoperative periprosthetic femur fracture is a known complication of total hip arthroplasty (THA) and a variety of cerclage systems are available to manage these fractures. The purpose of this study was to examine the in situ biomechanical response of cerclage systems for fixation of periprosthetic femur fractures that occur during cementless THA. We compared cobalt chrome (CoCr) cables, synthetic cables, monofilament wires and hose clamps under axial compressive and torsional loading. Metallic constructs with a positive locking system performed the best, supporting the highest loads with minimal implant subsidence (both axial and angular) after loading. Overall, the CoCr cable and hose clamp had the highest construct stiffness and least reduction in stiffness with increased loading. They were not demonstrably different from each other.

Intraoperative periprosthetic femur fracture is a known complication of total hip arthroplasty (THA). The incidence of intraoperative periprosthetic femur fracture has been reported to be between 0.1–1% for cemented [1,2] and 5.4% for uncemented primary THA [2], compared to 3.6–12.5% in cemented [2,3] and 8.8–45.9% in uncemented revision THA [1,2,4–7]. Risk factors for intraoperative periprosthetic femur fracture include the use of minimally invasive techniques [8], the use of press-fit cementless stems [1,2,4–6,8,9], revision operations [1,2,4–6,8,9], gender [8,9], bone loss or disease [3,5–8], and technical challenges at the time of the operation [8–15].

Treatment options for periprosthetic femur fractures in uncemented THA depend on the site of the fracture and the stability of the implant as well as surgeon preference and comfort [16]. A number of options have been proposed ranging from combinations of long stem femoral components, extramedullary fixation with cerclage cables, plates, and strut grafts [6–8,15,17]. Several studies have previously demonstrated differences in fixation technique and biomechanical advantages of various cerclage constructs in fixation of periprosthetic femur fractures [8,16–31]. Although metallic cerclage cables have been previously shown to provide more strength than twisted monofilament wire, cable use is associated with other complications and limitations in minimally invasive applications [18–22,32]. As a result, there has been a renewed interest in wire cerclage systems and newer materials such as synthetic cables have emerged as potential alternatives to traditional metallic cables [23–25,33–35].

The purpose of this study was to examine the in situ biomechanical response of cerclage systems for fixation of periprosthetic femur fractures that occur during cementless THA. We compared metallic cables, synthetic cables, monofilament wires and hose clamps under axial compressive and torsional rotational loading.

Methods

Femoral Preparation

Twenty-four large 4th generation composite femurs (model 3404, SawBones, Pacific Research Laboratories, Inc., Vashon, Washington) were used in this study. The femurs were prepared according to the manufacturer technique guide for an uncemented, tapered femoral stem (Zimmer M/L Taper, Warsaw, Indiana). A standard femoral neck osteotomy was performed with an oscillating saw at a height of 10 mm proximal to the lesser trochanter. A box punch and canal finder were inserted into the femur, followed by a lateralizing reamer. The femur was then broached sequentially to size 12.5. A periprosthetic fracture was created with a thin kerf blade (0.022 inch) band saw by placing the femur in a standardized jig and creating a longitudinal fracture extending 127 mm distally from the osteotomy plane. Using a band

One or more of the authors of this paper have disclosed potential or pertinent conflicts of interest, which may include receipt of payment, either direct or indirect, institutional support, or association with an entity in the biomedical field which may be perceived to have potential conflict of interest with this work. For full disclosure statements refer to http://dx.doi.org/10.1016/j.arth.2015.02.026.

Reprint requests: Nicholas B. Frisch, MD, MBA, Department of Orthopaedic Surgery, Henry Ford Hospital, 2799 West Grand Boulevard, CFP-6, Detroit, MI, 48202.

http://dx.doi.org/10.1016/j.arth.2015.02.026
0883-5403/

saw allowed for creation of a uniform and repeatable fracture pattern [32,36,37]. When considering intraoperative periprosthetic fractures, it has been suggested that the most common fracture pattern occurs from the level of the femoral neck down to the lesser trochanter, in the proximal 1/3 of the femur and as such our fracture modeled these previously reported patterns [1,6,14,15,28,29,38]. The femur was placed in a jig designed to standardize distal femur resection and the femoral condyles were resected 7 cm proximal to the distal end of the femur. The femur was then potted in custom made axial compression or torsional test fixtures using a two part epoxy filler and allowed to cure (Figs. 1 and 2).

Construct Preparation

The periprosthetic fracture was reduced using two cerclage constructs, one proximally at the level of the lesser trochanter and the other located 51 mm distal to the proximal position. This configuration was based on previously published reports and senior surgeon experience [24,29,37,39]. Tensioning of each construct was performed using the manufacturers' specification. Cobalt–chrome (CoCr) (1.6 mm Dall-Miles cables, Stryker) and synthetic cables (SuperCables, Kinamed, Camarillo, CA) were tensioned with the manufacturer tensioners. Hose clamp tensioning is engaged by a worm-screw so a torque limiting screw driver was used (25 in/lb). Monofilament wires (16 gauge stainless steel) were tensioned using an aeronautic safety wire twister (Milbar model 25W, Stride Tool, Glenwillow, OH). A total of six femurs were prepared for each of the four constructs: 1) CoCr cable, 2) hose clamp, 3) monofilament wire, and 4) synthetic cable (Fig. 1). After placement of the cerclage construct to reduce and fix the standardized fracture pattern, a size 12.5 femoral component (Zimmer M/L Taper, Warsaw, Indiana) with standard neck was impacted into the proximal femur and a 32 mm + 0 CoCr femoral head was impacted onto the trunnion. All constructs were prepared by the senior surgeon.

Axial Load Testing

Three femurs per construct type were selected for axial load testing. The potted distal end was clamped into the servohydraulic test frame (Model 8501M, Instron, Norwood, MA) and angulated at 25° of adduction and 0° of anteversion to approximate single-leg stance. At the proximal end, the femoral head of the implant interfaced with a hemicircular loading plate attached to the actuator applying the load. The axial tests were started by applying a 50 N preload followed by a loading rate of 0.8 mm/min. Axial load testing was terminated after a displacement of 20 mm.

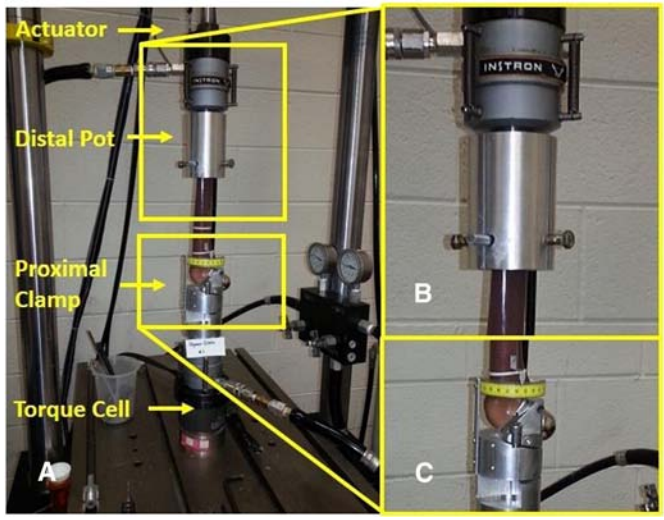

Fig. 2. Torsional test setup of femoral constructs. Note, the proximal femur is at the bottom of the figure and the distal femur is at the top. (A) Entire femoral construct installation in the Instron. (B) Detail of distal femur potting and interface to the Instron actuator. (C) Detail of proximal clamping and interface to the Instron torque cell.

The mechanical parameters that were measured during axial load testing included: subsidence onset and failure force, subsidence onset and failure displacement, stiffness, and total implant subsidence within the femur. The load–displacement histories are subdivided into two regions delineating the start of implant subsidence and characterized by two stiffnesses. Stiffness is defined as the slope of the linear part of the curve in these two regions. Subsidence onset force and displacement are defined as the intersection of the lines defining these two stiffnesses. Failure force and displacement were defined as the force maximum preceding a rapid force drop, indicative of hardware or femur failure. Total implant subsidence within the femur is defined as the difference between the failure displacement and the subsidence onset displacement. High definition video recorded during each trial was correlated with the biomechanical results on the force–displacement plots.

Comparisons of these parameters were then conducted between construct groups by one-way ANOVA and post-hoc Tukey–Kramer comparison except for the subsidence values, which were log transformed prior to statistical analysis due to failed normality tests. Regression analysis was used to determine the relationship between the total implant subsidence and the other mechanical parameters studied. The regression analysis is important because it indicates a relationship between

Fig. 1. Cerclage constructs.

Please cite this article as: Frisch NB, et al, Intraoperative Periprosthetic Femur Fracture: A Biomechanical Analysis of Cerclage Fixation, J Arthroplasty (2015), http://dx.doi.org/10.1016/j.arth.2015.02.026

the clinically detectable parameter, implant subsidence, and the mechanical test parameters, which identifies predictive links that may aid future implant design and performance.

Torsional Load

Three femurs per construct type were used in the torsional tests. The potted distal end of the femur was mounted to the rotary actuator while the proximal end was clamped around the head and neck of the implant and interfaced with a torque cell mounted to the test frame (Fig. 2). Rotational displacements were applied to the distal end and simulated the loading of an internally rotated femur during activities of rising from a seated position or stair climbing. Moments were applied at a rate of 2.4°/s and rotated through 40°. All constructs were taken to failure with the loading protocol.

Torque cell and actuator output were recorded during each test to capture the applied torque and rotation. A circumferential gauge was mounted to the proximal clamp and a dial attached to the proximal femur. The dial and gauge were used to determine the resultant angular subsidence of the implant stem relative to the femur.

The mechanical parameters of torque, rotational displacement, stiffness, and implant rotational subsidence were obtained from the applied torque and rotation data and collected during each test. Rotational subsidence, similar to axial subsidence, is the movement of the stem relative to the femur. This is different from rotational displacement which is the rotation of the entire construct. High definition video recorded during each trial was correlated with the biomechanical results on the torque–displacement plots.

Comparisons of these parameters were then conducted between construct groups by one-way ANOVA and post-hoc Tukey–Kramer comparison. Comparison between initial and final values was conducted using Student's t-test. Regression analysis was used to determine the relationship between the total angular subsidence and the other mechanical parameters studied. The regression analysis is important because it indicates a relationship between the clinically detectable parameter, implant subsidence, and the mechanical test parameters, which identifies predictive links that may aid future implant design and performance. A basic cost analysis was also performed.

Results

Axial Load

The typical load–displacement pattern for each construct is demonstrated in Fig. 3 (hose clamps, synthetic cables, and monofilament wires) and Fig. 4 (CoCr cables). In axial load testing, the constructs had load–displacement histories that exhibited two distinct loading regions (R1 and R2) with an associated stiffness (S1 and S2). The transition between R1 and R2 was delineated by an "elbow" in the load–displacement history, which corresponded to a decrease of the construct stiffness and the initiation of stem subsidence within the femur, verified by video analysis of individual tests. It was noted that the CoCr cable constructs exhibited three points on the load–displacement curve in which there was rapid displacement for the same applied load prior to catastrophic failure. Failure (i.e., the end of region R2) was determined to correspond with the first point of rapid displacement on the load–displacement curve.

Subsidence onset force and subsidence onset displacement were the force and displacement corresponding to the initiation of femoral stem subsidence within the femoral metaphysis. The mean subsidence onset force was 2548 N (±198 N SD) for hose clamps, 2501 N (±437 N SD) for CoCr cables, 1990 N (±426 N SD) for synthetic cables, and 1374 N (±550 N SD) for monofilament wire (Fig. 5). Mean subsidence onset force in the CoCr cables and hose clamps was greater than monofilament wires ($P < 0.05$). The mean subsidence onset displacement was 1.60 mm (±0.29 mm SD) for hose clamps, 1.66 mm (±0.70 mm SD) for CoCr cables, 2.04 mm (±0.58 mm SD) for synthetic cables, and 1.55 mm (±0.82 mm SD) for monofilament wire (Fig. 6). There were no statistical differences in subsidence onset displacement between cerclage constructs ($P > 0.05$).

Failure force and failure displacement were the force and displacement when there was catastrophic failure of the construct. The mean failure force was 9400 N for hose clamps, 7237 N for CoCr cables, 5781 N for synthetic cables, and 4010 N for monofilament wires. The differences in failure force all reached statistical significance ($P < 0.05$). The mean failure displacement was 10.86 mm (±1.32 mm SD) for hose clamps, 8.80 mm (±1.20 mm SD) for CoCr cables, 15.22 mm (±3.94 mm SD) for synthetic cables, and 18.61 mm (±1.18 mm SD) for monofilament wire (Fig. 6). The mean failure

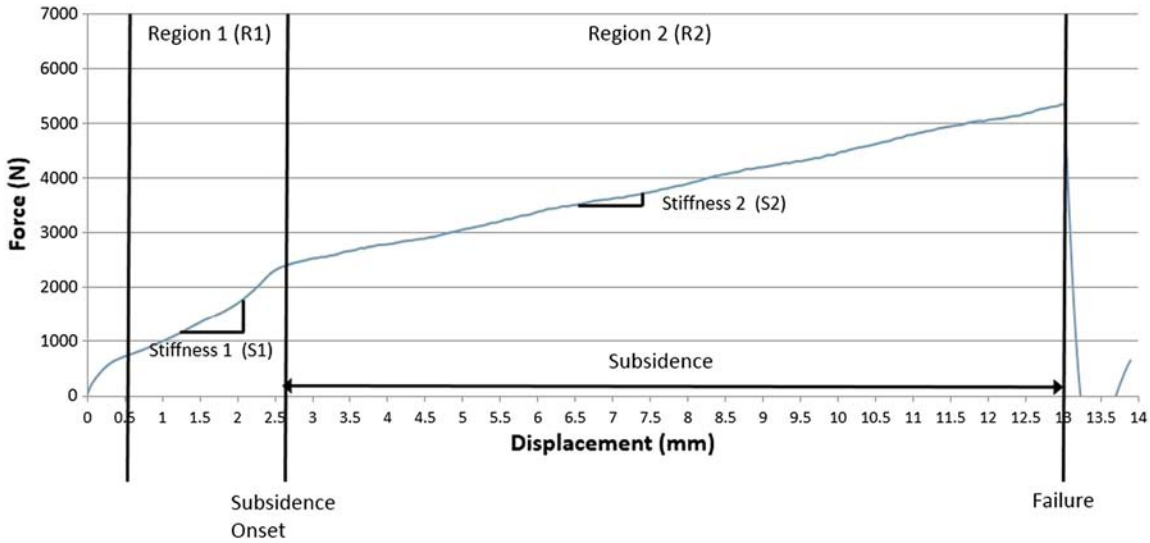

Fig. 3. Definition of mechanical parameters identified on load–displacement curve of the hose clamp, synthetic cable, and monofilament wire constructs. This curve is representative of the overall load displacement of these three constructs cumulatively, all 3 of which demonstrated a similar force–displacement curve pattern.

Please cite this article as: Frisch NB, et al, Intraoperative Periprosthetic Femur Fracture: A Biomechanical Analysis of Cerclage Fixation, J Arthroplasty (2015), http://dx.doi.org/10.1016/j.arth.2015.02.026

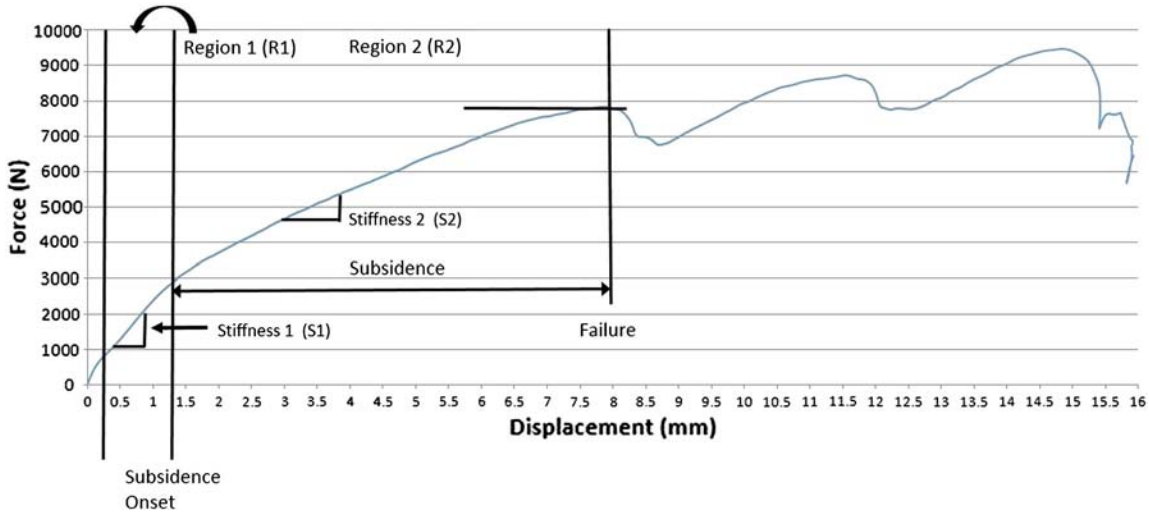

Fig. 4. Definition of mechanical parameters identified on load–displacement curve of the CoCr cable construct.

displacement of CoCr cables was lower than synthetic cables and monofilament wires ($P < 0.05$). The mean failure displacement of hose clamps was lower than monofilament wires ($P < 0.05$).

Construct stiffness was measured in the two different regions (R1 and R2) on the force-displacement plot, and a distinct reduction in construct stiffness was noted from R1 to R2. R1 stiffness was between 1153 N/mm and 1971 N/mm while the R2 stiffness ranged from 274 N/mm to 882 N/mm. In R1, there were no statistical differences ($P > 0.05$) in stiffness between cerclage constructs (Fig. 7). In R2, both hose clamps and CoCr cables had higher stiffness than the synthetic cables and monofilament wires ($P < 0.05$).

Total implant subsidence was measured as the displacement from the end of R1 when the implant began to subside to the catastrophic failure point at the end of R2. Mean total implant subsidence was 9.26 mm (±1.62 mm SD) for hose clamps, 7.14 mm (±0.57 mm SD) for CoCr cables, 13.18 mm (±3.46 mm SD) for synthetic cables, and 17.06 mm (±0.51 mm SD) for monofilament wire (Fig. 8). The total implant subsidence data failed tests of normality and were therefore log transformed to perform statistical tests. Total implant subsidence was lower in CoCr cables than in synthetic cables and monofilament wires ($P < 0.05$). Total implant subsidence was lower in hose clamps than in monofilament wires ($P < 0.05$).

A regression analysis was performed to evaluate the relationship between total implant subsidence and the several mechanical parameters discussed above. This showed that the subsidence onset force, failure force, and R2 stiffness were negatively associated to the subsidence displacement. Conversely, the subsidence and failure displacement had a positive relationship. All of the mechanical parameters (failure force, failure displacement, and R2 stiffness) in the subsiding region, R2, of the compression tests were significantly associated with total implant subsidence ($P < 0.05$). The only mechanical parameter in the pre-subsidence region, R1, which had a significant effect was the subsidence onset force ($P < 0.05$).

Torsional Load

The typical torque–displacement pattern for each construct is demonstrated in Fig. 9. In torsional load testing, 10 of the 12 cerclage constructs displayed torque–displacement histories that exhibited two distinct loading regions (R1 and R2) with an associated stiffness

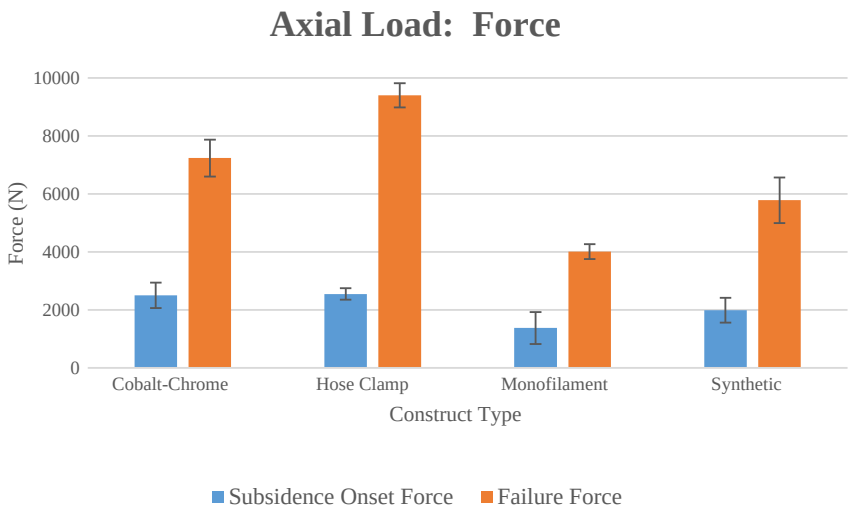

Fig. 5. Axial load subsidence onset and failure forces in the cerclage constructs. Subsidence onset force for monofilament wire was significantly less than cobalt–chrome and hose clamps ($P < 0.05$). Failure force was significantly different between all constructs ($P < 0.05$).

Please cite this article as: Frisch NB, et al, Intraoperative Periprosthetic Femur Fracture: A Biomechanical Analysis of Cerclage Fixation, J Arthroplasty (2015), http://dx.doi.org/10.1016/j.arth.2015.02.026

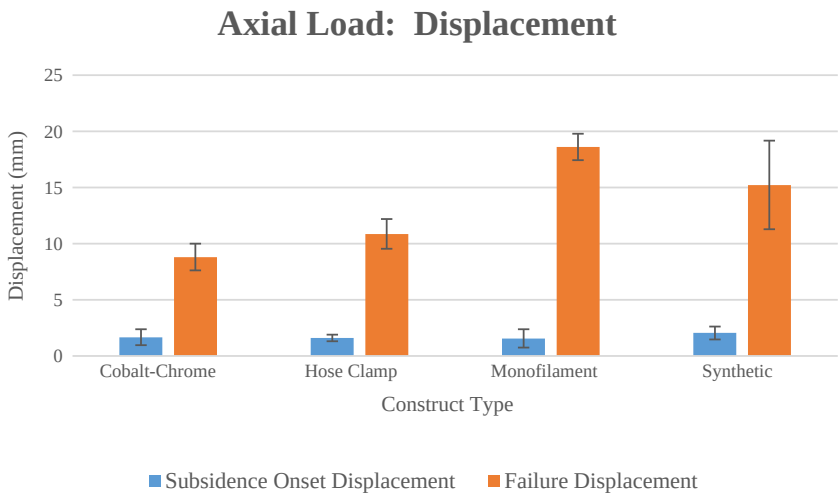

Fig. 6. Axial load subsidence onset displacement and failure displacement in the cerclage constructs. Failure displacement was significantly greater in monofilament wire and synthetic cable than in cobalt–chrome cable ($P < 0.05$). Failure displacement was significantly greater in monofilament wire than in hose clamps ($P < 0.05$).

(S1 and S2), which was similar to axial load testing. The transition between R1 and R2 was delineated by a sharp drop in the load–displacement history corresponding to spiral propagation of the simulated periprosthetic fracture. In the first torsional loading region (R1), failure started at the apex of the simulated periprosthetic fracture and progressed in a spiral pattern to the apex of the simulated fracture on the opposite side of either the medial or lateral fragment. The next torsional loading region (R2) ended when there was catastrophic failure of the femoral metaphysis. This was verified by video recordings of the individual tests. The two failures that did not follow these typical fracture events had a singular catastrophic failure of the femoral metaphysis. This occurred in one of the CoCr cable constructs and one of the hose clamp constructs. Lastly, the only cerclage cable that failed among all the tests was the proximal cable of one synthetic construct.

Initial failure torsion (T1) and rotational displacement occurred at the failure of either the medial or lateral fragment and prior to initiation of complete failure. Mean initial failure torsion (T1) was 41.28 Nm (±7.84 Nm SD) for hose clamps, 41.21 Nm (±0.93 Nm SD) for CoCr cables, 32.24 Nm (±3.42 Nm SD) for synthetic cables, and 28.21 Nm (±1.28 Nm SD) for monofilament wire (Fig. 10). T1 was higher in CoCr cables than in synthetic cables and monofilament wires ($P < 0.05$). T1 was higher in hose clamps than in monofilament wires ($P < 0.05$). There were no statistical differences ($P > 0.05$) in mean initial failure rotational displacement between cerclage constructs, which ranged from approximately 11°–12° (Fig. 11).

Failure torsion and rotational displacement occurred when there was catastrophic failure of the construct through the femoral metaphysis. Mean construct failure torsion (T2) was 37.75 Nm (±4.47 Nm SD) for hose clamps, 36.75 Nm (±2.77 Nm SD) for CoCr cables, 31.43 Nm (±1.53 Nm SD) for synthetic cables, and 29.86 Nm (±1.30 Nm SD) for monofilament wire (Fig. 10). T2 was higher in CoCr cables than in monofilament wires ($P < 0.05$). There were no statistical differences ($P > 0.05$) in mean failure rotational displacement between cerclage constructs (Fig. 11).

Mean initial (S1) and final construct rotational stiffness (S2) are depicted in Fig. 12. S1 of the hose clamp was greater than the synthetic cable ($P < 0.05$). S2 of the hose clamps and CoCr cables was greater than the monofilament wires ($P < 0.05$).

Mean total angular implant subsidence was 3.67° (±0.75° SD) for hose clamps, 6.77° (mean subsidence value not available due to lost data from measurement recording failure) for CoCr cables, 7.14° (±1.60° SD) for synthetic cables, and 5.76° (±1.15° SD) for monofilament wire. There were no statistical differences ($P > 0.05$) in total angular implant subsidence between cerclage constructs (CoCr construct not

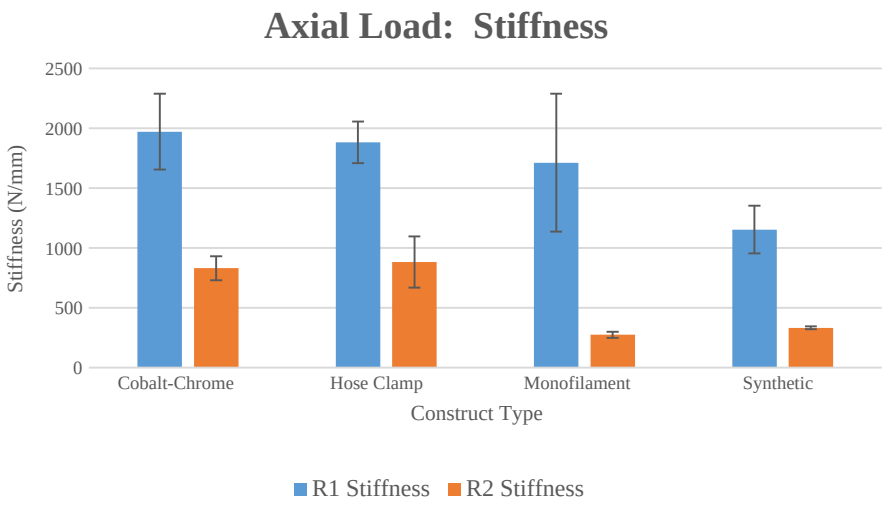

Fig. 7. Axial load region 1 and region 2 cerclage construct stiffness comparison. There were no significant differences in stiffness between the four constructs in R1. In R2, stiffness for cobalt–chrome cable and hose clamps were significantly greater than monofilament wire and synthetic cable ($P < 0.05$).

Please cite this article as: Frisch NB, et al, Intraoperative Periprosthetic Femur Fracture: A Biomechanical Analysis of Cerclage Fixation, J Arthroplasty (2015), http://dx.doi.org/10.1016/j.arth.2015.02.026

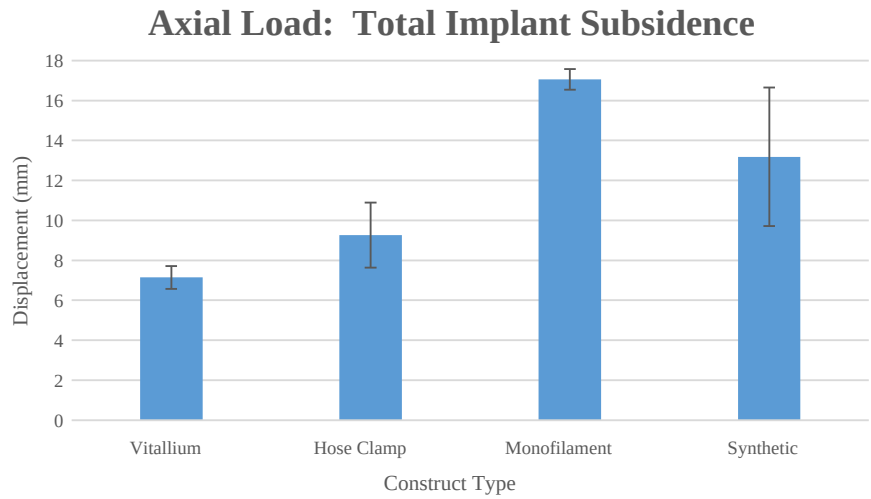

Fig. 8. Total implant subsidence for each of the cerclage constructs. Total implant subsidence was significantly less in cobalt–chrome cable than synthetic cable and monofilament wire ($P < 0.05$). Total implant subsidence was also significantly less in hose clamps than monofilament wire ($P < 0.05$).

included in this analysis). A regression analysis was used to evaluate the association between mean total angular implant subsidence and the mechanical parameters studied. Initial construct stiffness was the only mechanical parameter that reached statistical significance and it was found to be negatively associated with mean total angular implant subsidence ($P < 0.05$).

Discussion

The purpose of this study was to compare the biomechanical performance of multiple cerclage constructs for fixation of intraoperative periprosthetic femur fractures during cementless THA. Cable systems have been shown previously to have better biomechanical performance than wire systems [22,40]. However, metal cables have disadvantages such as metallic debris from their fragmentation and fraying, interruption of the cortical blood supply and, increased risk of injury and disease transmission to the surgeon from surgical glove punctures [27]. Nonmetallic cerclage applications have been utilized with encouraging results from both clinical [23] and in vivo animal studies [24,25]. Previous laboratory study of nonmetallic constructs has failed to demonstrate superiority over metallic cables [26,41]. Additionally, very little biomechanical information is available for intraoperative periprosthetic femur fractures repaired using synthetic cerclage cables in comparison with metallic cerclage systems. Although cerclage cable provides more strength than twisted monofilament wire, cable use can be more challenging in less invasive surgery as the cable crimping instrument cannot pass through a small incision [18–21]. The growing popularity of minimally invasive procedures has led to a renewed interest in wire cerclage systems. However, the clinical implications of reverting back to a biomechanically less stable fixation method have not been well vetted.

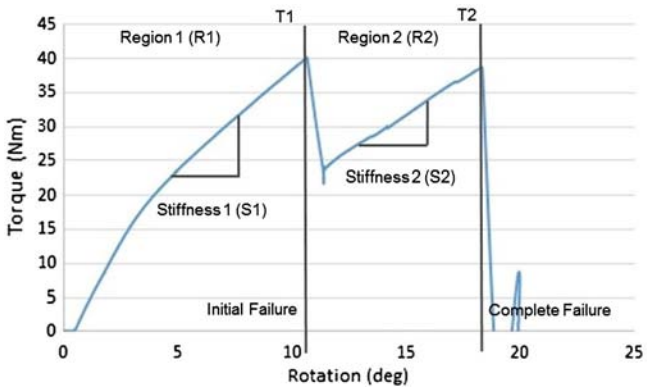

Fig. 9. Typical torque–rotation curve showing the two failure peaks. This curve is representative of the overall load displacement of these four constructs cumulatively, all 4 of which demonstrated a similar torque–displacement curve pattern.

Cable cerclage systems, whether metallic or synthetic, have a biomechanical advantage over twisted monofilament wire systems. For axial compression and torsion, CoCr cables were consistently stronger in both regions and stiffer throughout R2 than the monofilament wires. CoCr cables were also better at resisting implant migration. Synthetic cables had greater strength and higher stiffness than monofilament wires, but their significance was not detectable. This advantage may be associated with the positive locking mechanism in the cable construct design compared to the twisted monofilament wires. Clinically, however, the mechanical advantage of cable cerclage systems may be partially negated due to the challenges associated with using a crimping tool or mechanical fastening device. Other mechanical studies have suggested that the twist may be a source of weakness for monofilament wire fixation [25,42]. Video analysis during our study showing unwinding of the monofilament wires confirmed this failure mechanism, which began in R1 prior to the force or stiffness drop. Loosening of the other cerclage systems was prevented by the positive locking mechanism of their design as witnessed by the metallic cable slippage in the axially compressive loading tests and the synthetic cable breakage during one axially compressive test and one torsional test.

In light of metallic cable wear and injury disadvantages [27], nonmetallic cerclage applications have been considered and improved upon from earlier designs [23–26,41]. In situ biomechanical response of the synthetic cables proved to be as good as twisted monofilament wires. Their mechanical behavior exceeded that of monofilament wires, but statistical differences were not detected. Compared to the metallic cables, the nonmetallic cables exhibited reduced axially compressive strength and stiffness in R2. In torsion, the response was similar but not significant.

In our study, we determined the point of both initial and catastrophic failures of each device. Other studies have used different definitions for mechanical failure. Talbot et al defined failure when either 10 mm of displacement was reached (clinical failure) or when the first sudden 10% drop in load was observed after reaching a peak load (mechanical failure) [30]. For Lenz et al, construct failure was defined as axial displacement of more than 3 mm, with a stepwise system of loss of pretension, plastic deformation and then total failure [22]. Zdero et al used catastrophic failure and clinical failure [37]. A construct was considered

Please cite this article as: Frisch NB, et al, Intraoperative Periprosthetic Femur Fracture: A Biomechanical Analysis of Cerclage Fixation, J Arthroplasty (2015), http://dx.doi.org/10.1016/j.arth.2015.02.026

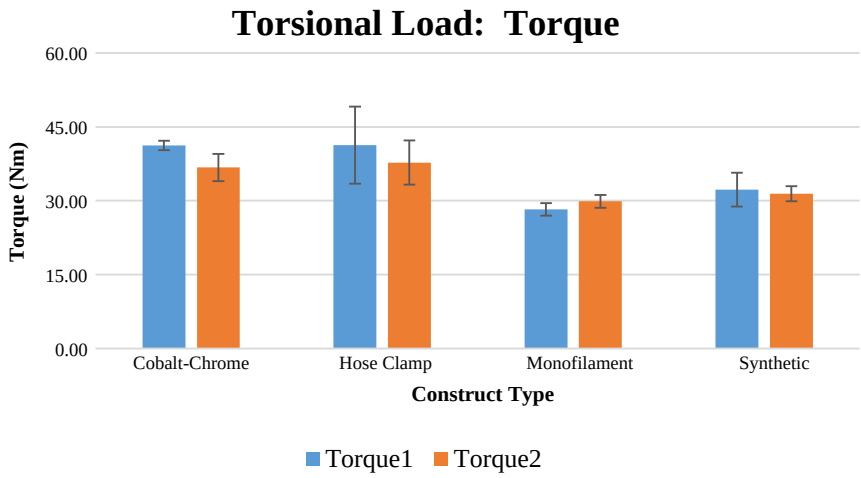

Fig. 10. Construct initial failure torque (T1) and catastrophic failure torque (T2). Monofilament wire and synthetic cable had significantly lower torque 1 than cobalt–chrome cable ($P < 0.05$). Monofilament wire had significantly lower torque 1 than hose clamp ($P < 0.05$).

to have undergone "clinical failure" when either 10 mm of vertical deflection was reached (which is a clinically practical limit) or when the first abrupt decrease in applied force was experienced after reaching a peak load (which was deemed to indicate substantial initial structural collapse). Catastrophic failure was often a transverse femoral break near the support base (three of five specimens) or an oblique break at the most distal screw (one of five specimens), occurred in most specimens.

There is no doubt that a catastrophic bone failure is clinically relevant. The axially compressive and torsion experiments in this study exhibited construct subsidence prior to failure of the simulated bone, most notably in the axially compressive tests. From above, axial subsidence may have a threshold value of 10 mm of construct displacement. While all cerclage systems subsided in both test regimes of this study, in the case of axial subsidence, the synthetic cables and monofilament wires exceed this threshold within our axial test regime. This raises the question whether failure is the onset of subsidence or the final subsidence displacement. Our monotonic failure tests allow us to analyze which mechanical parameters are associated with the extent of subsidence so that we can use that data to evaluate those future cyclic tests that would be conducted below the onset of subsidence. It should be noted that the onset of subsidence is greater than average body weight for all cerclage systems. As a result, the main difference between the two test regimes was the mechanical parameter that best predicted the subsidence of the implant. The initial force, or subsidence force, in the compression tests was associated with the level of subsidence that was observed in the implant. The initial construct stiffness in the torsional tests was associated with the amount of implant displacement relative to the femur. While this is different between the two test regimens, it does provide a predictor to the degree of implant subsidence prior to the subsidence yield point and without having to test beyond that threshold.

If subsidence is taken to be a clinically relevant event, then it is important to find predictive mechanical parameters in the region prior to its onset and to understand if the construct retains stability afterwards. Stiffness provides a measure of construct stability. All cerclage systems saw a reduction in stiffness from R1 to R2. Metallic cables retained this stability to a greater extent than the synthetic and monofilament wires in R2. This is important because once the construct has reached region R2, it has already had initial failure. Clinically, this may result in an implant which is loose and needs revision. If this is the case, then the region R1 data are more relevant clinically, and one could argue that there are few clinical differences between the constructs. However, additional clinical testing is needed to make this determination.

Hose clamps are commercially available products that have been used for over 100 years in other industries such as automotive, mechanical and aeronautics. However, they are not FDA approved for this application and are not implantable devices. Their long track record in other

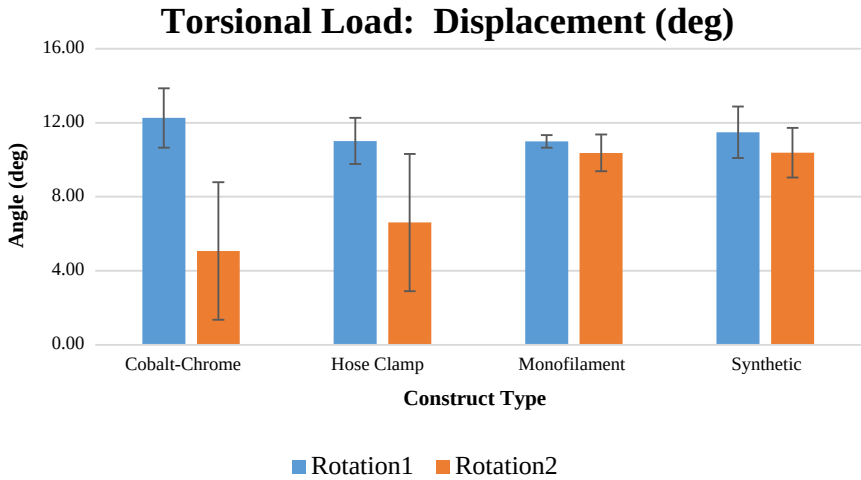

Fig. 11. Construct failure rotations. Rotation 1 defined as initial failure angular displacement and Rotation 2 defined as catastrophic failure angular displacement.

Please cite this article as: Frisch NB, et al, Intraoperative Periprosthetic Femur Fracture: A Biomechanical Analysis of Cerclage Fixation, J Arthroplasty (2015), http://dx.doi.org/10.1016/j.arth.2015.02.026

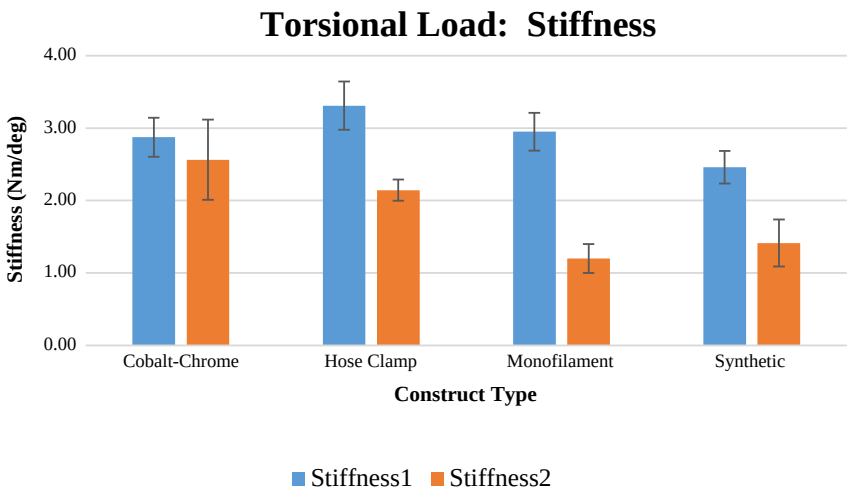

Fig. 12. Construct stiffness. Synthetic cable had significantly less stiffness in region 1 than hose clamps ($P < 0.05$). Monofilament wire had significantly less stiffness than cobalt–chrome cable and hose clamp in region 2 ($P < 0.05$).

industries makes them a valuable control for other cerclage fixation devices. Previous studies have demonstrated the use of hose clamps for both clinical and biomechanical purposes. Chandler et al described using hose clamps clinically for temporary fixation for allograft struts during periprosthetic fracture fixation [43]. The strength of these hose clamps has made them popular for temporary support while permanent fixation is being applied. Liu et al compared the compressive forces of hose clamps with monofilament wires and metallic cables [44]. They identified the advantages of temporary use with allograft or with cementation of femoral stem into a femur during revision procedures utilized extended trochanteric osteotomies.

This study has several limitations. While synthetic femurs have been shown to model good bone stock relatively well, they cannot be broadly applicable to osteoporotic and lower quality bone. With a synthetic femur, there is no way to assess the impact of soft tissue involvement, which may in practice limit cerclage application and play a role in overall wound healing. This testing looked specifically at axial load and torsional load testing, but in vivo the effect of cyclical loading, which was not tested, may become significant. It is important to differentiate intraoperative and postoperative periprosthetic fracture patterns and in this study we attempted to recreate a pattern consistent with intraoperative fractures that start proximally and extend distally below the lesser trochanter during femur preparation and implant placement. They do not apply for all fracture patterns, including for example those that are more distal fracture or fractures associated with significant comminution. The implant used in this study was a standard M/L taper stem. While geometric design of the stem may differ between manufacturers, the results should be broadly applicable to all press-fit stems as the axial and torsional loading would similarly open the simulated fracture due to wedging or twisting of the stem based on the nature of these designs. It would not necessarily apply to cemented stems or longer, diaphyseal fixation designs.

Conclusion

The purpose of this study was to determine the biomechanical performance of cerclage constructs in fixation of intraoperative periprosthetic fractures during cementless THA in both axial load and torsional load testing. Metallic constructs with a positive locking system performed the best—these supported the highest loads with minimal implant subsidence (both axial and angular) after loading. Overall, the CoCr cable and hose clamp had the highest construct stiffness and least reduction in stiffness with increased loading. They were not demonstrably different from each other.

Acknowledgments

The authors would like to thank Yener N. Yeni, Ph.D., Head, Section of Biomechanics, Bone and Joint Center, Henry Ford Hospital, Henry Ford Health System for his support of this project.

References

1. Kavanagh BF. Femoral fractures associated with total hip arthroplasty. Orthop Clin North Am 1992;23(2):249.
2. Berry DJ. Epidemiology: hip and knee. Orthop Clin North Am 1999;30(2):183.
3. Davis III CM, Berry DJ, Harmsen WS. Cemented revision of failed uncemented femoral components of total hip arthroplasty. J Bone Joint Surg Am 2003;85-A(7):1264.
4. Malkani AL, Lewallen DG, Cabanela ME, et al. Femoral component revision using an uncemented, proximally coated, long-stem prosthesis. J Arthroplast 1996;11(4):411.
5. Egan KJ, Di Cesare PE. Intraoperative complications of revision hip arthroplasty using a fully porous-coated straight cobalt-chrome femoral stem. J Arthroplast 1995(10 Suppl.):S45.
6. Masri BA, Meek RM, Duncan CP. Periprosthetic fractures evaluation and treatment. Clin Orthop Relat Res 2004;420:80.
7. Meek RM, Garbuz DS, Masri BA, et al. Intraoperative fracture of the femur in revision total hip arthroplasty with a diaphyseal fitting stem. J Bone Joint Surg Am 2004;86-A(3):480.
8. Davidson D, Pike J, Garbuz D, et al. Intraoperative periprosthetic fractures during total hip arthroplasty. Evaluation and management. J Bone Joint Surg Am 2000;90(9):2008.
9. Nowak M, Kusz D, Wojciechowski P, et al. Risk factors for intraoperative periprosthetic femoral fractures during the total hip arthroplasty. Pol Orthop Traumatol 2012;77:59.
10. Savin L, Barharosie C, Botez P. Periprosthetic femoral fractures—evaluation of risk factors. Rev Med Chir Soc Med Nat Iasi 2012;116(3):846.
11. Cook RE, Jenkins PJ, Walmsley PJ, et al. Risk factors for periprosthetic fractures of the hip: a survivorship analysis. Clin Orthop Relat Res 2008;466(7):1652.
12. Cross MB, Nam D, van der Meulen MC, et al. A rare case of a bisphosphonate-induced peri-prosthetic femoral fracture. J Bone Joint Surg Br 2012;94(7):994.
13. Dhawan RK, Mangham DC, Graham NM. Periprosthetic femoral fracture due to biodegradable cement restrictor. J Arthroplast 2012;27(8):1581.e13.
14. Berend KR, Lombardi Jr AV. Intraoperative femur fracture is associated with stem and instrument design in primary total hip arthroplasty. Clin Orthop Relat Res 2010;468(9):2377.
15. Berend KR, Lombardi Jr AV, Mallory TH, et al. Cerclage wires or cables for the management of intraoperative fracture associated with a cementless, tapered femoral prosthesis: results at 2 to 16 years. J Arthroplast 2004;19(7 Suppl. 2):17.
16. Beals RK, Tower SS. Periprosthetic fractures of the femur. An analysis of 93 fractures. Clin Orthop Relat Res 1996(327):238.
17. Pike J, Davidson D, Garbuz D, et al. Principles of treatment for periprosthetic femoral shaft fractures around well-fixed total hip arthroplasty. J Am Acad Orthop Surg 2009;17(11):677.
18. Apivatthakakul T, Phornphutkul C. Percutaneous cerclage wiring for reduction of periprosthetic and difficult femoral fractures. A technical note. Injury 2012;43(6):966.
19. Apivatthakakul T, Phornphutkul C, Bunmaprasert T, et al. Percutaneous cerclage wiring and minimally invasive plate osteosynthesis (MIPO): a percutaneous reduction technique in the treatment of Vancouver type B1 periprosthetic femoral shaft fractures. Arch Orthop Trauma Surg 2012;132(6):813.

Please cite this article as: Frisch NB, et al, Intraoperative Periprosthetic Femur Fracture: A Biomechanical Analysis of Cerclage Fixation, J Arthroplasty (2015), http://dx.doi.org/10.1016/j.arth.2015.02.026

20. Ehlinger M, Adam P, Di Marco A, et al. Periprosthetic femoral fractures treated by locked plating: feasibility assessment of the mini-invasive surgical option. A prospective series of 36 fractures. Orthop Traumatol Surg Res 2011;97(6):622.
21. Ehlinger M, Bonnomet F, Adam P. Periprosthetic femoral fractures: the minimally invasive fixation option. Orthop Traumatol Surg Res 2010;96(3):304.
22. Lenz M, Perren SM, Richards RG, et al. Biomechanical performance of different cable and wire cerclage configurations. Int Orthop 2013;37(1):125.
23. Tountas AA, Kwok JM, Kugler M. The Partridge nylon cerclage: its use as a supplementary fixation of difficult femoral fractures in the elderly. J Orthop Trauma 1990;4(3):299.
24. Stromberg L, Karlstrom G. The influence of nylon cerclage on diaphyseal bone strength: an experimental evaluation of Partridge bands on rabbits. Orthopedics 1986;9(2):237.
25. Rhinelander FW, Stewart CL. Experimental fixation of femoral osteotomies by cerclage with nylon straps. Clin Orthop Relat Res 1983(179):298.
26. Shaw JA, Daubert HB. Compression capability of cerclage fixation systems. A biomechanical study. Orthopedics 1988;11(8):1169.
27. Silverton CD, Jacobs JJ, Rosenberg AG, et al. Complications of a cable grip system. J Arthroplast 1996;11(4):400.
28. Dennis MG, Simon JA, Kummer FJ, et al. Fixation of periprosthetic femoral shaft fractures: a biomechanical comparison of two techniques. J Orthop Trauma 2001; 15(3):177.
29. Dennis MG, Simon JA, Kummer FJ, et al. Fixation of periprosthetic femoral shaft fractures occurring at the tip of the stem: a biomechanical study of 5 techniques. J Arthroplast 2000;15(4):523.
30. Talbot M, Zdero R, Schemitsch EH. Cyclic loading of periprosthetic fracture fixation constructs. J Trauma 2008;64(5):1308.
31. Demos HA, Briones MS, White PH, et al. A biomechanical comparison of periprosthetic femoral fracture fixation in normal and osteoporotic cadaveric bone. J Arthroplast 2012;27(5):783.
32. Lever JP, Zdero R, Nousiainen MT, et al. The biomechanical analysis of three plating fixation systems for periprosthetic femoral fracture near the tip of a total hip arthroplasty. J Orthop Surg Res 2010;5:45.
33. Edwards TB, Stuart KD, Trappey GJ, et al. Utility of polymer cerclage cables in revision shoulder arthroplasty. Orthopedics 2011;34(4):264.
34. Rothaug PG, Boston RC, Richardson DW, et al. A comparison of ultra-high-molecular weight polyethylene cable and stainless steel wire using two fixation techniques for repair of equine midbody sesamoid fractures: an in vitro biomechanical study. Vet Surg 2002;31(5):445.
35. Canet F, Baril Y, Brailovski V, et al. Force relaxation and sprinback of novel elastic orthopedic cables. Conf Proc IEEE Eng Med Biol Soc 2011;2011:5758.
36. Choi JK, Gardner TR, Yoon E, et al. The effect of fixation technique on the stiffness of comminuted Vancouver B1 periprosthetic femur fractures. J Arthroplast 2010;25(6 Suppl.):124.
37. Zdero R, Walker R, Waddell JP, et al. Biomechanical evaluation of periprosthetic femoral fracture fixation. J Bone Joint Surg Am 2008;90(5):1068.
38. Gulsen M, Karatosun V, Uyulgan B. The biomechanical assessment of fixation methods in periprosthetic femur fractures. Acta Orthop Traumatol Turc 2011; 45(4):266.
39. Han SM. Comparison of wiring techniques for bone fracture fixation in total hip arthroplasty. Tohoku J Exp Med 2000;192(1):41.
40. Lindahl H, Oden A, Garellick G, et al. The excess mortality due to periprosthetic femur fracture. A study from the Swedish national hip arthroplasty register. Bone 2007;40(5):1294.
41. Kirby BM, Wilson JW. Knot strength of nylon-band cerclage. Acta Orthop Scand 1989; 60(6):696.
42. Harnroongroj T. Twist knot cerclage wire: the appropriate wire tension for knot construction and fracture stability. Clin Biomech (Bristol, Avon) 1998;13(6):449.
43. Chandler HP, Tigges RG. The role of allografts in the treatment of periprosthetic femoral fractures. Instr Course Lect 1998;47:257.
44. Liu Y, Lu S, Liu B. The reason and management of intraoperative femur fracture during hip arthroplasty. Zhonghua Wai Ke Za Zhi 1998;36(2):93.

Please cite this article as: Frisch NB, et al, Intraoperative Periprosthetic Femur Fracture: A Biomechanical Analysis of Cerclage Fixation, J Arthroplasty (2015), http://dx.doi.org/10.1016/j.arth.2015.02.026